# Molecular Profiling of Salivary Gland Intraductal Carcinoma Revealed a Subset of Tumors Harboring *NCOA4-RET* and Novel *TRIM27-RET* Fusions

## *A Report of 17 cases*

*Alena Skálová, MD, PhD,* Tomas Vanecek, PhD,*† Emmanuelle Uro-Coste, MD, PhD,‡§ Justin A. Bishop, MD, PhD,‖ Ilan Weinreb, MD,¶ Lester D.R. Thompson, MD,# Stefano de Sanctis, MD, PhD,** Marco Schiavo-Lena, MD,†† Jan Laco, MD, PhD,‡‡ Cécile Badoual, MD, PhD,§§ Thalita Santana Conceiçao, DDS, MSc, PhD,‖‖ Nikola Ptáková, MSc,† Martina Baněčkova, MD,* Marketa Miesbauerová, MD,* and Michal Michal, MD**

**Abstract:** Intraductal carcinoma (IC) is the new World Health Organization designation for tumors previously called "low-grade cribriform cystadenocarcinoma" and "low-grade salivary duct carcinoma." The relationship of IC to salivary duct carcinoma is controversial, but they now are considered to be distinct entities. IC is a rare low-grade malignant salivary gland neoplasm with features similar to mammary atypical ductal hyperplasia or ductal carcinoma in situ, that shows diffuse S100 protein and mammaglobin positivity and is only partially defined genetically. (Mammary analogue) secretory carcinoma harboring *ETV6-NTRK3*, and in rare cases *ETV6-RET* fusion, shares histomorphologic and immunophenotypical features with IC. Recently, *RET* rearrangements and *NCOA4-RET* have been described in IC, suggesting a partial genetic overlap with mammary analogue secretory carcinoma. Here, we genetically characterize the largest cohort of IC to date to further explore this relationship. Seventeen cases of IC were analyzed by next-generation sequencing using the FusionPlex Solid Tumor kit (ArcherDX). Identified fusions were confirmed using fluorescence in situ hybridization break apart and, in some cases, fusion probes, and a reverse transcription polymerase chain reaction designed specifically to the detected breakpoints. All analyzed cases were known to be negative for *ETV6* rearrangement by fluorescence in situ hybridization and for *ETV6-NTRK3* fusion by reverse transcription polymerase chain reaction. Next-generation sequencing analysis detected a *NCOA4-RET* fusion transcript joining exon 7 or 8 of *NCOA4* gene and exon 12 of *RET* gene in 6 cases of intercalated duct type IC; and a novel *TRIM27-RET* fusion transcript between exons 3 and 12 in 2 cases of salivary gland tumors displaying histologic and immunohistochemical features typical of apocrine IC. A total of 47% of IC harbored a fusion involving *RET*. In conclusion, we have confirmed the presence of *NCOA4-RET* as the dominant fusion in intercalated duct type IC. A novel finding in our study has been a discovery of a subset of IC patients with apocrine variant IC harboring a novel *TRIM27-RET*.

**Key Words:** salivary gland neoplasm, intraductal carcinoma, cystadenocarcinoma, mammary analogue secretory carcinoma, MASC, *NCOA4-RET*, *TRIM27-RET*, *RET*-targeted therapy

(*Am J Surg Pathol* 2018;42:1445–1455)

From the *Department of Pathology, Charles University, Faculty of Medicine in Plzen; †Molecular and Genetic Laboratory, Biopticka Laboratory Ltd, Plzen; ‡‡The Fingerland Department of Pathology, Charles University, Faculty of Medicine and University Hospital, Hradec Kralove, Czech Republic; ‡Department of Pathology, Toulouse University Hospital; §INSERM U1037, Cancer Research Center of Toulouse (CRCT), Toulouse; §§Department of Pathology, G. Pompidou Hospital, Paris, APHP, Paris Descartes University, Paris, France; ‖Department of Pathology, UT Southwestern Medical Center, Dallas, TX; ¶Department of Pathology, University Health Network, Toronto, ON, Canada; #Southern California Permanente Medical Group, Woodland Hills, CA; **Histopathology Department, Addenbrooke Hospital, Cambridge University Hospitals NHS Trust, Cambridge, UK; ††Department of Pathology, IRCCS San Raffaele Scientific Institute, Milan, Italy; and ‖‖Department of Oral Pathology, Faculty of Dentistry, University of São Paulo, São Paulo, Brazil.

The preliminary results of the study were presented as a platform presentation at USCAP Meeting 2018, Vancouver, Canada, March 17-22, 2018 (A.S.).

Conflicts of Interest and Source of Funding: Supported in parts by the grant SVV–2018 No. 260 391 provided by the Ministry of Education Youth and Sports of the Czech Republic. The authors have disclosed that they have no significant relationships with, or financial interest in, any commercial companies pertaining to this article.

Correspondence: Alena Skálová, MD, PhD, Sikl's Department of Pathology, Medical Faculty of Charles University, Faculty Hospital, E. Benese 13, Plzen 305 99, Czech Republic (e-mail: skalova@fnplzen.cz).



Secretory carcinoma of the salivary glands, also known as mammary analogue secretory carcinoma (MASC), was originally described by Skálová et al, in 2010.[1] Most of these tumors were previously categorized as acinic cell carcinoma,[2–4] adenocarcinoma not otherwise specified or low-grade cystadenocarcinoma, but were recognized as a

distinct entity based on their morphologic and molecular resemblance to secretory carcinoma of the breast,[1] and subsequently adopted by the World Health Organization (WHO) Classification of Head and Neck Tumours in 2017 as secretory carcinoma of salivary glands.[5] MASCs are characterized by abundant eosinophilic cytoplasm and secretions, consistent immunohistochemical positivity for S100 and mammaglobin, and recurrent *ETV6-NTRK3* gene fusions. Increasing experience with MASCs, however, has also highlighted a small subset of cases that demonstrate divergent molecular findings.[6,7] Most notably, Skálová et al,[8] recently characterized 10 cases with alternate *ETV6-RET* fusion.

Intraductal carcinoma (IC) is the new WHO designation for tumors previously called "low-grade cribriform cystadenocarcinoma" and "low-grade salivary duct carcinoma."[9] The relationship of IC to salivary duct carcinoma (SDC) has been controversial, but recently they are considered to be distinct entities. IC is a rare low-grade malignant salivary gland neoplasm with features similar to mammary atypical ductal hyperplasia or ductal carcinoma in situ, that shows diffuse S100 protein and mammaglobin positivity and an intact myoepithelial cell layer decorated by p63 protein, calponin, and cytokeratin 14.

MASC has many architectural and immunophenotypic features similar to, or identical with IC. Both tumors may share diffuse S100 protein and mammaglobin positivity and similar architectural features, such as cribriform-like secretory spaces, multicystic architecture and papillary growth pattern.[1] These 2 morphologically similar entities should be, however, strictly separated. Pure IC is an in situ lesion with no capacity for metastasizing while MASC does not have any significant intraductal component and may metastasize. Most importantly, the neoplastic nests and cysts of IC are completely surrounded by a rim of non-neoplastic myoepithelial cells, which are positive for p63 protein, and other myoepithelial cell-related markers such as smooth muscle actin, CK14, and calponin. Thus, immunohistochemistry is helpful in differential diagnosis between IC and MASC; with p63 protein expression providing evidence of intact myoepithelial layer in IC while virtually negative in MASC.

Weinreb et al,[10] recently demonstrated recurrent rearrangements involving *RET* in 47% of ICs with an intercalated duct phenotype and confirmed *NCOA4-RET* fusion in one such case using next-generation sequencing (NGS) and direct sequencing. Dogan et al,[11] presented, however, at the USCAP Annual Meeting on March 6th 2017 as a poster, *NCOA4-RET* fusion in one of 4 tumors morphologically and immunophenotypically compatible with MASC using the NGS assay. The proposed novel finding of *NCOA4-RET* fusion in MASC attracted our attention as it was in contrast with our experience. So far, we have tested $>300$ cases of MASC and never found any other fusion than *ETV6-NTRK3* or *ETV6-RET*.[1,8]

There have been only limited genomic and immunohistochemical comparative studies of pure IC and MASC, so far. One case of "low-grade cribriform cystadenocarcinoma" tested as part of the control group in the original description of MASC was *ETV6* negative by fluorescence in situ hybridization (FISH).[1] A second study found one case of "low-grade cribriform cystadenocarcinoma" to be *ETV6* negative by FISH.[12] A recent third study also showed *ETV6* negativity by FISH in 5 cases of IC tested.[13] In the study by Shah et al,[14] there was a single case originally classified as MASC that was negative to *ETV6* break by FISH, and positive for S100 and mammaglobin by immunohistochemistry, re-classified as IC on review. The study by Weinreb et al,[10] also found no evidence of *ETV6* rearrangement in any of their IC cases tested, and did not confirm the partner gene for *RET* in the majority of the tumors. Therefore, we used a comprehensive genetic analysis to examine the largest cohort of IC to date, with the goal of defining the most common gene fusions and potentially identifying novel fusions.

## MATERIALS AND METHODS

Among more than 6200 cases of primary salivary gland tumors, 16 cases of IC were retrieved from the consultation files of the Salivary Gland Tumor Registry, at the Department of Pathology, Faculty of Medicine in Plzen, and Biopticka Laboratory Ltd, Plzen, Czech Republic (A.S. and M.M.). Interestingly, 7 cases were originally diagnosed as MASCs by referring pathologists, and sent as consults for molecular confirmation. One additional case of predominantly apocrine IC was added which was originally reported as case no. 15 in Weinreb et al,[10] and tested by NGS.

The histopathologic features of all tumors and the immunohistochemical stains, when available, were reviewed by 2 pathologists (A.S. and M.B.). A diagnosis of IC was confirmed in cases that displayed histologic features consistent with original description in conjunction with the appropriate immunohistochemical profile, that is, co-expression of S100 protein, cytokeratin CK7, and mammaglobin in the absence of DOG1 staining. Moreover, an intact myoepithelial layer decorated by p63 and/or CK14 and calponin provided evidence of intraductal component. Widely invasive carcinomas were excluded. Tumors were classified further into 2 groups, according to criteria published recently[10]: those that showed an intercalated duct phenotype and those with an apocrine phenotype. This was determined both histologically and immunohistochemically. Thus, a total number of 17 IC cases were studied by NGS using ArcherDX FusionPlex kit.

For conventional microscopy, the excised tissues were fixed in formalin, routinely processed, embedded in paraffin (FFPE), cut, and stained with hematoxylin and eosin. In most cases, additional stains were also performed, including periodic acid-Schiff with and without diastase, mucicarmine, and Alcian blue at pH 2.5.

For immunohistochemical analysis, 4-μm-thick sections were cut from paraffin blocks and mounted on positively charged slides (TOMO, Matsunami Glass IND, Japan). Sections were processed on a BenchMark ULTRA (Ventana Medical System, Tucson, AZ), deparaffinized and then subjected to heat-induced epitope retrieval by immersion in a CC1 solution at pH 8.6 at 95°C. All

**TABLE 1.** Antibodies Used for Immunohistochemical Study

| Antibody Specificity | Clone | Dilution | Antigen Retrieval/ Time (min) | Source |
|---|---|---|---|---|
| S100 protein | Polyclonal | RTU | CC1/20 | Ventana |
| Mammaglobin | 304-1A5 | RTU | CC1/36 | DakoCytomation |
| CK7 | OV-TL 12/30 | 1:200 | CC1/36 | DakoCytomation |
| p63 | 4A4 | RTU | CC1/64 | Ventana |
| DOG1 | SP31 | RTU | CC1/36 | Cell Marque |
| GATA-3 | L50-823 | 1:200 | CC1/52 | BioCareMedical |
| SOX-10 | Polyclonal | 1:100 | CC1/64 | Cell Marque |
| MIB1 | 30-9 | RTU | CC1/64 | Ventana |
| Androgen receptor | SP107 | RTU | CC1/64 | Cell Marque |
| Calponin | EP798Y | RTU | CC1/36 | Cell Marque |
| CK 14 | SP53 | RTU | CC1/64 | Cell Marque |

CC1—EDTA buffer, pH 8.6.
RTU indicates ready to use.

other primary antibodies used are summarized in Table 1. The bound antibodies were visualized using the ultraView Universal DAB Detection Kit (Roche) and ultraView Universal Alkaline Phosphatase Red Detection Kit (Roche). The slides were counterstained with Mayer's hematoxylin. Appropriate positive and negative controls were employed.

Where available, clinical follow-up was obtained from the patients, their physicians, or from referring pathologists.

## Molecular Genetic Study

### Sample Preparation for NGS and Reverse Transcriptase Polymerase Chain Reaction

For NGS and reverse transcriptase polymerase chain reaction (RT-PCR) analysis, 2 to 3 FFPE sections (10 μm thick) were macrodissected to isolate tumor-rich regions. Samples were extracted for total nucleic acid using Agencourt FormaPure Kit (Beckman Coulter, Brea, CA) following the corresponding protocol with an overnight digest and an additional 80°C incubation as described in modification of the protocol by ArcherDX (ArcherDX Inc., Boulder, CO). RNA component of the total nucleic acid was quantified using the Qubit Broad Range RNA Assay Kit (Thermo Fisher Scientific) and 2 μL of sample.

### RNA Integrity Assessment and Library Preparation for NGS

Unless otherwise indicated, 250 ng of FFPE RNA was used as input for NGS library construction. To assess RNA quality, the PreSeq RNA QC Assay using iTaq Universal SYBR Green Supermix (Biorad, Hercules, CA) was performed on all samples during library preparation to generate a measure of the integrity of RNA (in the form of a cycle threshold [Ct] value). Library preparation and RNA QC were performed following the Archer FusionPlex Protocol for Illumina (ArcherDX Inc.). The Archer FusionPlex Solid Tumor Kit was used. Final libraries were diluted 1:100,000 and quantified in a 10 μL reaction following the Library Quantification for Illumina Libraries protocol and assuming a 200 bp fragment length (KAPA, Wilmington, MA). The concentration of final libraries was around 200 nM. Threshold representing the minimum molar concentration for which sequencing can be robustly performed was set at 50 nM.

### NGS Sequencing and Analysis

Libraries were sequenced on a NextSeq. 500 sequencer (Illumina, San Diego, CA). They were diluted to 4 nM and equal amounts of up to 16 libraries were pooled per run. The optimal number of raw reads per sample was set to 3,000,000. Library pools were diluted to 1.8 pM library stock spiked with 20% PhiX and loaded in the NextSeq MID cartridge. Analysis of sequencing results was performed using the Archer Analysis software (v5; ArcherDX Inc.). Fusion parameters were set to a minimum of 5 valid fusion reads with a minimum of 3 unique start sites within the valid fusion reads.

### FISH Analysis of RET Break and TRIM27-RET Fusion

Four micrometer thick FFPE sections were placed onto positively charged slides. Hematoxylin and eosin–stained slides were examined for determination of areas for cell counting.

The unstained slides were routinely deparaffinized and incubated in the ×1 Target Retrieval Solution Citrate pH 6 (Dako, Glostrup, Denmark) at 95°C for 40 minutes and subsequently cooled for 20 minutes at room temperature in the same solution. Slides were washed in deionized water for 5 minutes and digested in protease solution with Pepsin (0.5 mg/mL) (Sigma Aldrich, St. Louis, MO) in 0.01 M HCl at 37°C for 35 to 60 minutes according the sample conditions. Slides were then placed into deionized water for 5 minutes, dehydrated in a series of ethanol solution (70%, 85%, 96% for 2 min each) and air-dried.

For the detection of *RET* rearrangement, factory premixed commercial probe ZytoLight SPEC RET Dual Color Break Apart Probe (ZytoVision GmbH, Bremerhaven, Germany) have been used. For the *TRIM27-RET* dual-fusion detection custom designed SureFISH probe (Agilent Technologies Inc., Santa Clara with chromosomal regions chr6:28631476-29131075 and chr10:43354893-43849282 have been used. Probe-mixture for the fusion detection was prepared from corresponding probes (each color was delivered in separated well), deionized water and LSI Buffer (Vysis/Abbott Molecular) in a 1:1:1:7 ratio, respectively.

An appropriate amount of mixed and premixed probes was applied on specimens, covered with a glass coverslip and sealed with rubber cement. Slides were incubated in the ThermoBrite instrument (StatSpin/Iris Sample Processing, Westwood, MA) with codenaturation at 85°C/8 minutes and hybridization at 37°C/16 hours. Rubber cemented coverslip was then removed and the slide was placed in post-hybridization wash solution (2×SSC/0.3% NP-40) at 72°C/2 minutes. The slide was air-dried in the dark, counterstained with 4′, 6′-diamidino-2-phenylindole DAPI (Vysis/Abbott Molecular), cover slipped and immediately examined.

**TABLE 2.** Primers for RT-PCR Analysis

| Primer Name | Sequence 5′-3′ |
|---|---|
| NCOA4-RET-7-12-F | CCCTTCCTGGAGAAGAGAGG |
| NCOA4-RET-7-12-R | GTACCCTGCTCTGCCTTTCA |
| NCOA4-RET-8-12-F | TACCCAAAAGCAGACCTTGG |
| NCOA4-RET-8-12-R | CGCCTTCTCCTAGAGTTTTTCC |
| TRIM27-RET-3-12-F | TGATCGCTCAGCTAGAAGAGAA |
| TRIM27-RET-3-12-R | CCAAGTTCTTCCGAGGGAAT |

## FISH Interpretation

The sections were examined with an Olympus BX51 fluorescence microscope (Olympus Corporation, Tokyo, Japan) using a ×100 objective and filter sets Triple Band Pass (DAPI/SpectrumGreen/SpectrumOrange), Dual Band Pass (SpectrumGreen/SpectrumOrange) and Single Band Pass (SpectrumGreen or SpectrumOrange).

For each probe, 100 randomly selected nonoverlapping tumor cell nuclei were examined for the presence of yellow or green and orange fluorescent signals. Regarding break-apart probe, yellow signals were considered negative, separate orange and green signals were considered as positive; conversely for fusion probe, yellow signals were considered positive, separate orange and green signals were considered as negative. Cut-off values for break apart and fusion probes were set to <10% and 20% of nuclei with chromosomal breakpoint and fusion signals, respectively (mean+3 SD in normal non-neoplastic control tissues).

## RT-PCR Analysis of NCOA4-RET and TRIM27-RET Fusion Transcripts

Two microliter of cDNA prepared by standard RT procedure using Transcriptor First Strand cDNA Synthesis Kit (RNA input 500 ng) (Roche Diagnostics, Mannheim, Germany) was added to reaction consisted of 12.5 μL of HotStar Taq PCR Master Mix (QIAgen, Hilden, Germany), 10 pmol of each fusion specific primer (Table 2) and distilled water up to 25 μL. The amplification program comprised denaturation at 95°C for 14 minutes and then 45 cycles of denaturation at 95°C for 1 minute, annealing at temperature 55°C for 1 minute and extension at 72°C for 1 minute. The program was finished by incubation at 72°C for 7 minutes.

**TABLE 3.** Detailed Molecular Findings of 17 Cases of Salivary Gland ICs

| No. | Age/ Sex | Diagnosis | NGS | Exons Joining | FISH RET ba | FISH TRIM27-RET Fusion | RT-PCR Fusion Specific | FISH ETV6 ba | RT-PCR ETV6-NTRK3 |
|---|---|---|---|---|---|---|---|---|---|
| 1 | 38/M | Pure IC intercalated duct type, solid microcystic, rich lymphoid stroma | NCOA4-RET | 8-12 | Positive* | ND | Positive | Negative | Negative |
| 2 | 47/M | Pure IC intercalated duct type, solid multicystic, "MASC-like" | NCOA4-RET | 7-12 | Positive* | ND | Positive | Negative | Negative |
| 3 | 54/M | IC with apocrine features, micropapillary, minimal invasion | TRIM27-RET | 3-12 | Positive | Positive | Positive | Negative | Negative |
| 4 | 50/M | Pure IC intercalated duct type, solid multicystic, "MASC-like" | NA | — | NA | ND | Negative | Negative | Negative |
| 5 | 58/M | Pure IC intercalated duct type, solid microcystic, apocrine, papillary | NA | — | NA | ND | ND | NA | Negative |
| 6 | 81/M | Pure IC intercalated duct type, "roman bridges" Invasive component of epithelial-myoepithelial carcinoma | NA | — | Negative | ND | Negative | Negative | Negative |
| 7† | 50/F | Pure IC intercalated duct type, unicystic | Negative | — | Negative | ND | ND | Negative | Negative |
| 8 | 74/M | Pure IC intercalated duct type, papillary, multicystic | NCOA4-RET | 8-12 | Positive* | ND | Positive | Negative | Negative |
| 9 | 36/F | Pure IC intercalated duct type, few apocrine cells | Negative | — | Negative | ND | ND | Negative | Negative |
| 10 | 53/F | IC intercalated duct type, minimal invasion | Negative | — | Negative | ND | ND | Negative | Negative |
| 11 | 75/F | IC with apocrine features, papillary, thick fibrous capsule | Negative | — | Negative | ND | ND | Negative | Negative |
| 12 | 69/M | IC with apocrine features, unicystic | Negative | — | ND | ND | ND | ND | Negative |
| 13 | 42/F | Pure IC intercalated duct type, unicystic | Negative | — | ND | ND | ND | Negative | Negative |
| 14 | 61/F | Pure IC intercalated duct type, solid, microcystic, "MASC-like" | NCOA4-RET | 7-12 | Positive* | ND | Positive | Negative | Negative |
| 15 | 36/M | Pure IC intercalated duct type, solid, microcystic, "MASC-like" | NCOA4-RET | 8-12 | Positive* | ND | Positive | NA | Negative |
| 16 | 50/M | Pure IC intercalated duct type, solid, microcystic, "MASC-like" | NCOA4-RET | 8-12 | Positive | ND | Positive | ND | ND |
| 17‡ | 66/M | IC with widespread apocrine features, and hybrid intercalated duct pattern | TRIM27-RET | 3-12 | Positive | Positive | Positive | ND | ND |

*Cases 1 to 2, 8, and 14 to 16 showed a *RET* FISH signal pattern indicative of an inversion/rearrangement (in one allele a gap between orange and green signals was observed, hovewer this gap didnot reach internal cut-off (≥2 signal diameters apart).

†Published in Laco et al.[22]

‡Published as case no.15 in Weinreb et al.[10]

F indicates female; M, male; NA, not analyzable; ND, not done.

Successfully amplified PCR products were purified with magnetic particles Agencourt AMPure (Agencourt Bioscience Corporation, A Beckman Coulter Company, Beverly, MA). Products were then bi-directionally sequenced using Big Dye Terminator Sequencing kit (Applied Biosystems, Foster City, CA), purified with magnetic particles Agencourt CleanSEQ (Agencourt Bioscience Corporation), all according to manufacturer's protocol and run on an automated sequencer ABI Prism 3130×l (Applied Biosystems) at a constant voltage of 13.2 kV for 11 minutes.

## RESULTS

### Molecular Genetic Findings

The 17 cases of IC were analyzed by NGS using the ArcherDX analysis platform. This analysis detected a *NCOA4-RET* fusion transcript joining exon 7 or 8 of *NCOA4* gene and exon 12 of *RET* gene in 6 cases and a novel *TRIM27-RET* fusion transcript between exons 3 and 12 in 2 cases of salivary gland tumors displaying histologic and immunohistochemical features typical of apocrine IC (Table 3). The fusion transcripts were confirmed by RT-PCR and sequencing (Figs. 1A–C). FISH analysis using *RET* break-apart probe showed 2 different patterns, one "negative" when distance criteria was used according to the interpretation rules, but still showing small separation of signals (cases 1 to 2, 8, and 14 to 16) (Fig. 2A), and a regular break (classic positive pattern) with apparent separation of signals demonstrated in 2 cases (cases 3 and 17) (Fig. 2B). Confirmation using FISH *TRIM27-RET* fusion probe displayed fusion signals with amplification (Fig. 2C). Localization of *RET*, *NCOA4*, and *TRIM27* genes for an explanation of 2 different patterns of FISH break-apart results is shown in the figure (Fig. 2D).

All analyzed cases were negative for *ETV6-NTRK3* gene fusion by the FusionPlex kit, RT-PCR, and *ETV6* gene was found intact by FISH (Table 3). No other fusion transcripts different from *NCOA4-RET* or *TRIM27-RET* were found by NGS in any analyzable case of IC. A total of 47% of analyzed cases harbored a *RET* fusion by NGS, an identical finding to that found by Weinreb et al.[10] By RT-PCR, the fusions *NCOA4-RET* and *TRIM27-RET* were confirmed in all NGS positive cases. The *RET* FISH break-apart probe and


**FIGURE 1.** Schematic representation of the fusion transcripts with Sanger sequence of RT-PCR. *NCOA4-RET* exons 7 and 12 (A), *NCOA4-RET* exons 8 and 12 (B), *TRIM27-RET* exons 3 and 12 (C).

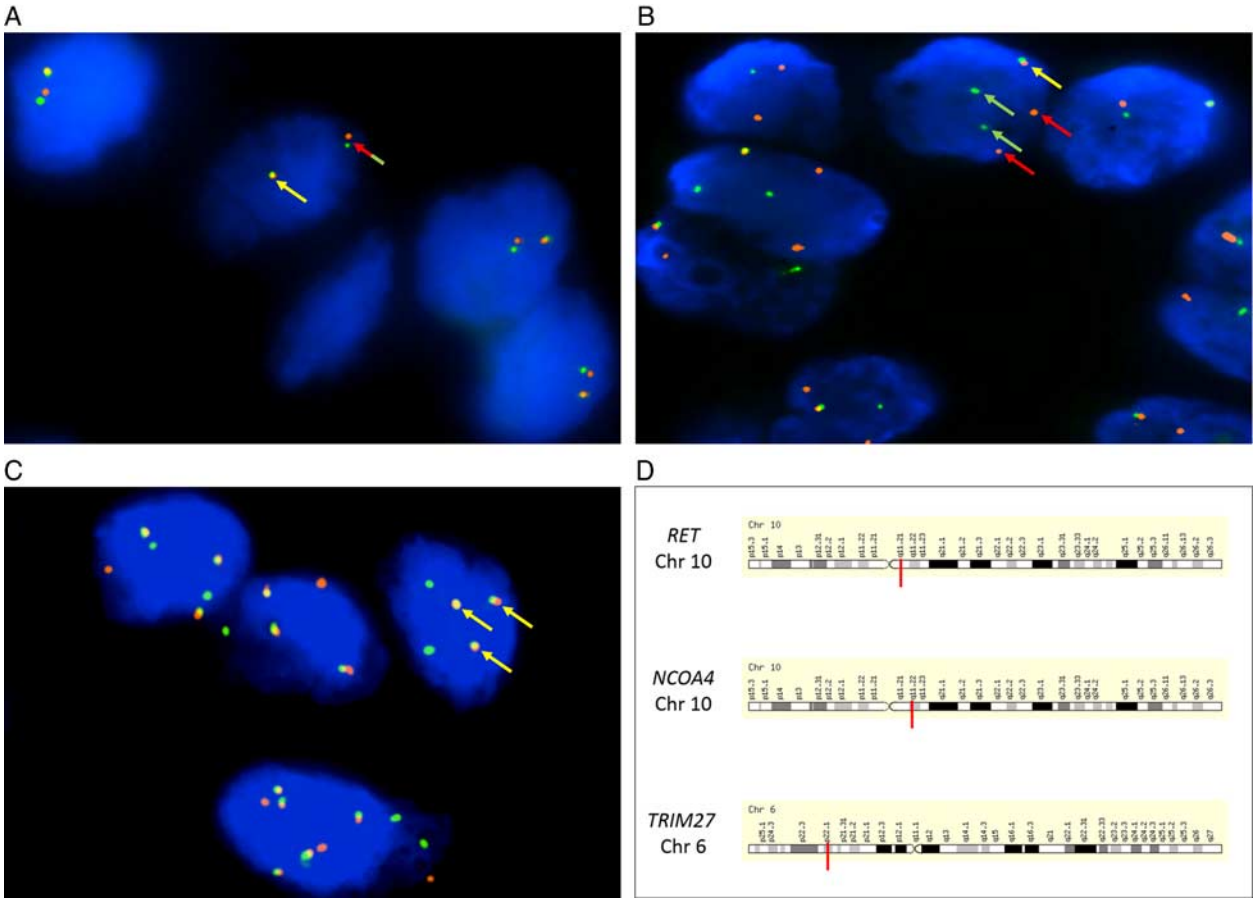


**FIGURE 2.** FISH analysis. A, Seemingly negative *RET* break-apart probe with small separation of signals (red-green arrow). B, Regular *RET* break-apart probe positivity (red and green arrows); yellow arrows show intact gene in both cases. C, *TRIM27-RET* fusion probe positivity with signal amplification (yellow arrows). D, Scheme of chromosomal localization of *RET*, *NCOA4*, and *TRIM27* genes.

*TRIM27-RET* fusion probe successfully detected the *RET* rearrangement in both cases with *TRIM27-RET*. "False" negative FISH results were obtained in all *NCOA4-RET* cases for *RET* rearrangement owing to this fusion being the result of an intrachromosomal rearrangement with inversion. Although a narrow separation of the FISH signals was noted in each case. The molecular findings are summarized in Table 3.

## Clinical and Histologic Characteristics of the Study Group

The study cohort consisted of 15 pure ICs and 2 ICs with limited microinvasion. The patients with available clinical information included 11 males and 6 females, with a wide age-range at diagnosis of 36 to 81 years (mean, 55.3 y). The most common anatomic site of involvement was the parotid gland (no. = 16 patients), with one case in the buccal mucosa. The tumors ranged from 0.6 to 4.6 cm (mean, 1.64 cm). Detailed clinical, follow-up, and histologic findings in 17 patients with IC are summarized in Table 4.

Grossly, the tumors were entirely circumscribed and encapsulated in most cases, although infiltrative edges were seen in 2 cases. All tumors were treated by surgical excision with clear surgical margins. Five patients underwent subtotal conservative parotidectomy (cases 2, 8, 14 and 15), followed by radiation therapy (case 8), and cervical lymph node dissection (case 2), respectively. Clinical follow-up data were obtained from 15 patients, and ranged from 8 months to 15 years (mean, 5 y and 5 mo); 2 patients were lost to follow-up.

## Microscopic and Immunohistochemical Features

Histologically, at low power magnification, most cases were well-circumscribed and encapsulated. Focal areas with microinvasion were seen in 2 cases of IC (case 3 and 10). In addition, in case 6 the tumor of parotid gland was a hybrid lesion composed of 2 separate components, one was invasive epithelial-myoepithelial carcinoma and the other pure IC without invasion. Lymphovascular and perineural invasion was absent in all cases. All tumors were characterized by luminal epithelial proliferations with ductal phenotype arranged mainly in multiple cystic patterns, besides solid and cribriform islands (Fig. 3A). Intracystic growth often formed micropapillary structures with anastomosing and filigreed epithelial tufts, comprising the so called Roman-bridges pattern (Fig. 3B). Eosinophilic proteinaceous secretion and hemorrhagic areas were occasionally observed in some cystic spaces, as well as

**TABLE 4.** Clinicopathologic Features of 16 Cases of Salivary Gland Intraductal Carcinomas

| No. | Age/ Sex | Site | Size (cm) | Diagnosis | Nuclear Grade | S100 Protein/ MGA | AR | Treatment | Outcome (in months) |
|---|---|---|---|---|---|---|---|---|---|
| 1 | 38/M | Parotid | 4.0 | Pure IC intercalated duct type, solid microcystic, rich lymphoid stroma | Low | +/+ | − | Superficial parotidectomy | 20 NED |
| 2 | 47/M | Parotid | 1.4 | Pure IC intercalated duct type, solid multicystic, "MASC-like" | Low | +/+ | − | Parotidectomy and neck dissection | 36 NED |
| 3 | 54/M | Parotid | 2.2 | IC with apocrine features, micropapillary, minimal invasion | High | +/+ | + | Superficial parotidectomy | 8 NED |
| 4 | 50/M | Parotid | 1.0 | Pure IC intercalated duct type, solid multicystic, "MASC-like" | Low | +/+ | − | Partial parotidectomy | 57 NED |
| 5 | 58/M | Parotid | 1.5 | Pure IC intercalated duct type, solid microcystic, apocrine, papillary | Low | +/+ | + | Wide excision | 144 NED |
| 6 | 81/M | Parotid | NA | Pure IC intercalated duct type, "roman-bridges" Invasive component of epithelial-myoepithelial carcinoma* | Low | +/ND | − | NA | NA |
| 7 | 50/F | Parotid | 1.5 | Pure IC intercalated duct type, unicystic | Low | +/+ | − | Wide excision | 72 NED |
| 8 | 74/M | Parotid | 1.5 | Pure IC intercalated duct type, papillary, multicystic | Low | +/+ | − | Parotidectomy and radiotherapy | 62 NED |
| 9 | 36/F | Buccal mucosa | 0.6 | Pure IC intercalated duct type, few apocrine cells | Low | +/+ | ND | Wide excision | 180 NED |
| 10 | 53/F | Parotid | 2.0 | IC intercalated duct type, minimal invasion | Low | +/+ | − | Parotidectomy | 180 NED |
| 11 | 75/F | Parotid | 4.6 | IC with apocrine features, papillary, thick fibrous capsule | Intermediate | +/+ | ND | Parotidectomy | 72 NED |
| 12 | 69/M | Parotid | 0.9 | IC with apocrine features, unicystic | Low | +/ND | ND | Parotidectomy | 60 NED |
| 13 | 42/F | Parotid | 0.7 | Pure IC intercalated duct type, unicystic | Low | +/ND | ND | Parotidectomy | 60 NED |
| 14 | 61/F | Parotid | 1.5 | Pure IC intercalated duct type, solid, microcystic, "MASC-like" Focal necrosis | Low | +/+ | − | Partial parotidectomy (deep lobe) | 8 NED |
| 15 | 36/M | Parotid | 1.0 | Pure IC intercalated duct type, solid, microcystic, "MASC-like" | Low | +/+ | − | Partial parotidectomy | 8 NED |
| 16 | 50/M | Parotid | 2.5 | Pure IC intercalated duct type, solid, microcystic, "MASC-like" | Low | +/+ | − | Partial parotidectomy | 12 NED |
| 17* | 66/M | Parotid | 1.3 | IC with widespread apocrine features, and hybrid intercalated duct pattern | Intermediate | +/+ | + | NA | NA |

*Published as case no.15 in Weinreb et al.[10]
F indicates female; MGA, mammaglobin; M, male; NA, not available; ND, not done; NED, no evidence of disease.

cholesterol clefts and foamy histiocytes. Tumor stroma was densely collagenized in 3 cases, while in one case there was rich lymphoid stroma with a growth pattern similar to Warthin tumor (case 1) (Fig. 3C).

On high-power magnification, all cases showed bland cytology, with tumor cells ranging from small to medium size, with indistinct cell borders, showing round or ovoid nuclei with dark condensed or finely dispersed chromatin and large pale to eosinophilic cytoplasm. Mitoses were inconspicuous and only in one case there were focal comedo necrosis (case 14). Tumor cells showed lipofuscin-like brown pigment within cells intracytoplasmic vacuoles in most cases (Fig. 3D). Six cases showed focal (cases 5, 9) or extensive apocrine differentiation (cases 3, 11, 12, 17) (Fig. 4A).

In ICs with apocrine and mixed hybrid growth patterns (6/17), most tumor cells were positive for androgen receptor (AR) (Fig. 4B). All examined IC cases were positive for S100 protein (Fig. 5A), mammaglobin (Fig. 5B), and SOX-10 (Fig. 5C), typically in a strong and diffuse manner. An intact myoepithelial cell layer surrounding tumor islands was evidenced by p63 immunohistochemical expression (which was negative in other tumor cells) (Fig. 5D). Calponin, and CK 14 decorated an intact peripheral myoepithelial cell layer in all examined cases, as well. Staining for DOG1 was negative in most cases, with limited areas of positive cells in one case. Proliferative activity was generally low, with a mean MIB1 index <5% (range 1% to 10%).

## DISCUSSION

The term "intraductal carcinoma" of the salivary gland was first introduced in 1983 by Chen[15] in a description of a single case arising in minor salivary gland of the oral cavity. Subsequently, several case reports and small series of the same tumor entity were published with various names, including "low-grade salivary duct carcinoma,"[16,17] and "low-grade cribriform cystadenocarcinoma."[18] These all referred to a combination of cystic and solid structures of varying size formed by intraductal epithelial proliferation composed of cells resembling intercalated ductal cells and structures similar to atypical ductal hyperplasia and ductal carcinoma in situ of breast. In the current WHO classification, this tumor is now again regarded as an IC.[9]

IC has been surrounded by controversy since its discovery not only because of variable terminologies, but mainly because of its uncertain relationship to SDC.[16–19]

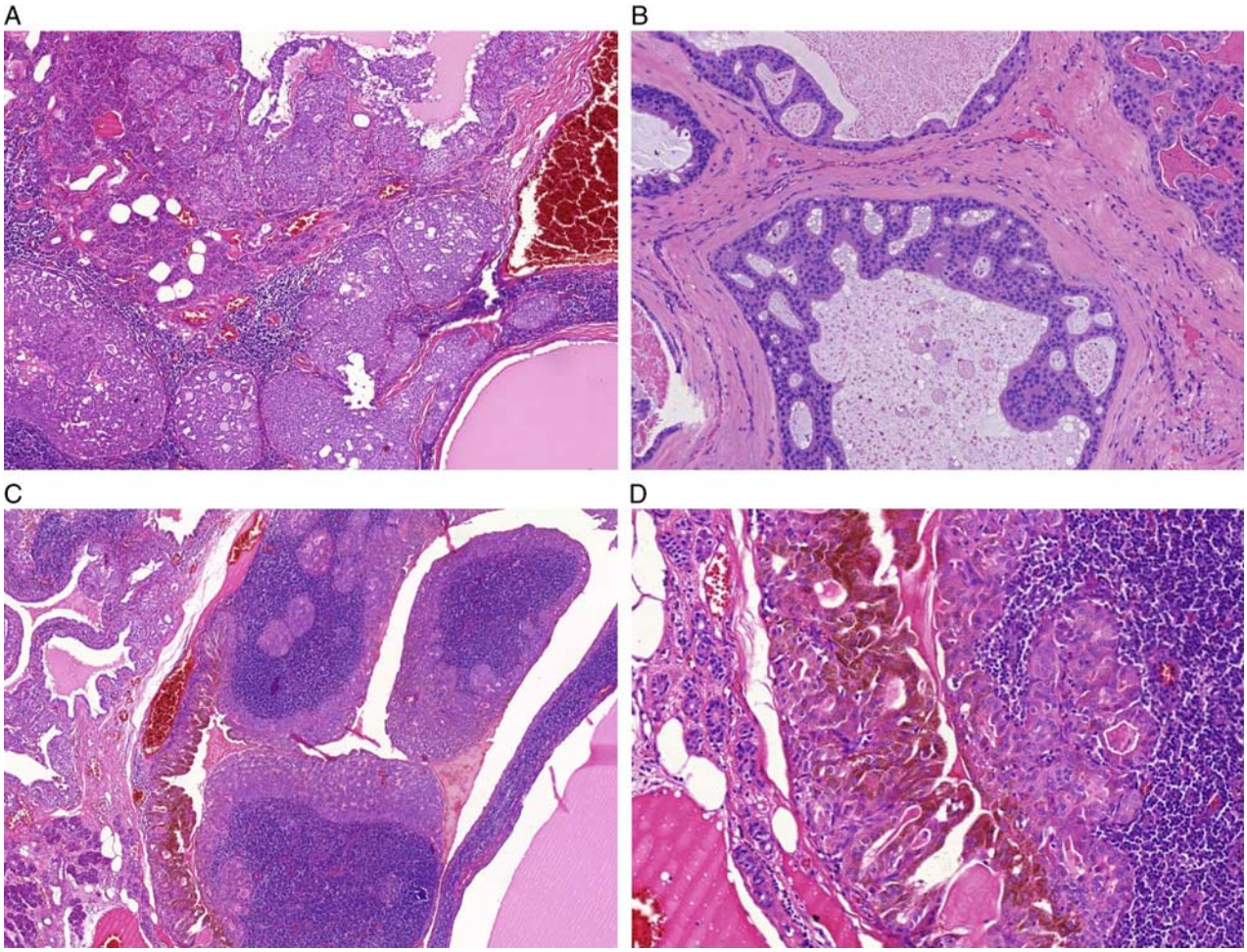


**FIGURE 3.** IC, intercalated duct type. A, All tumors were characterized by luminal epithelial proliferations with ductal phenotype arranged mainly in multiple cystic patterns, besides solid and cribriform islands. B, Intracystic growth often formed micropapillary structures with anastomosing and filigreed epithelial tufts, comprising the so called Roman-bridges pattern. C, There was rich lymphoid stroma with growth pattern similar to Warthin tumor in case 1. D, Tumor cells showed lipofuscin-like brown pigment within cells intracytoplasmic vacuoles in most cases.

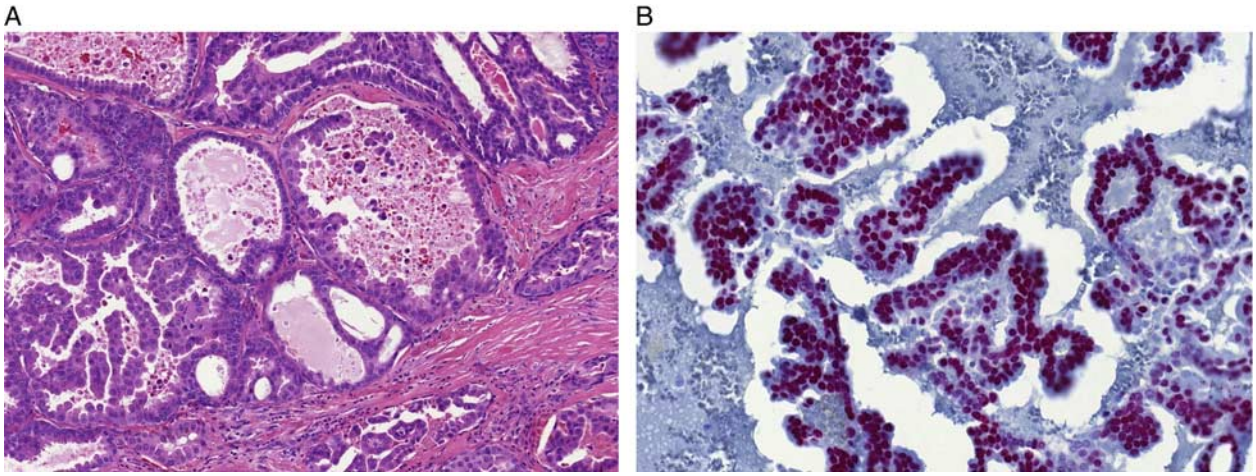


**FIGURE 4.** IC, apocrine variant. IC with widespread apocrine differentiation (A). Most tumor cells were positive for AR (B).

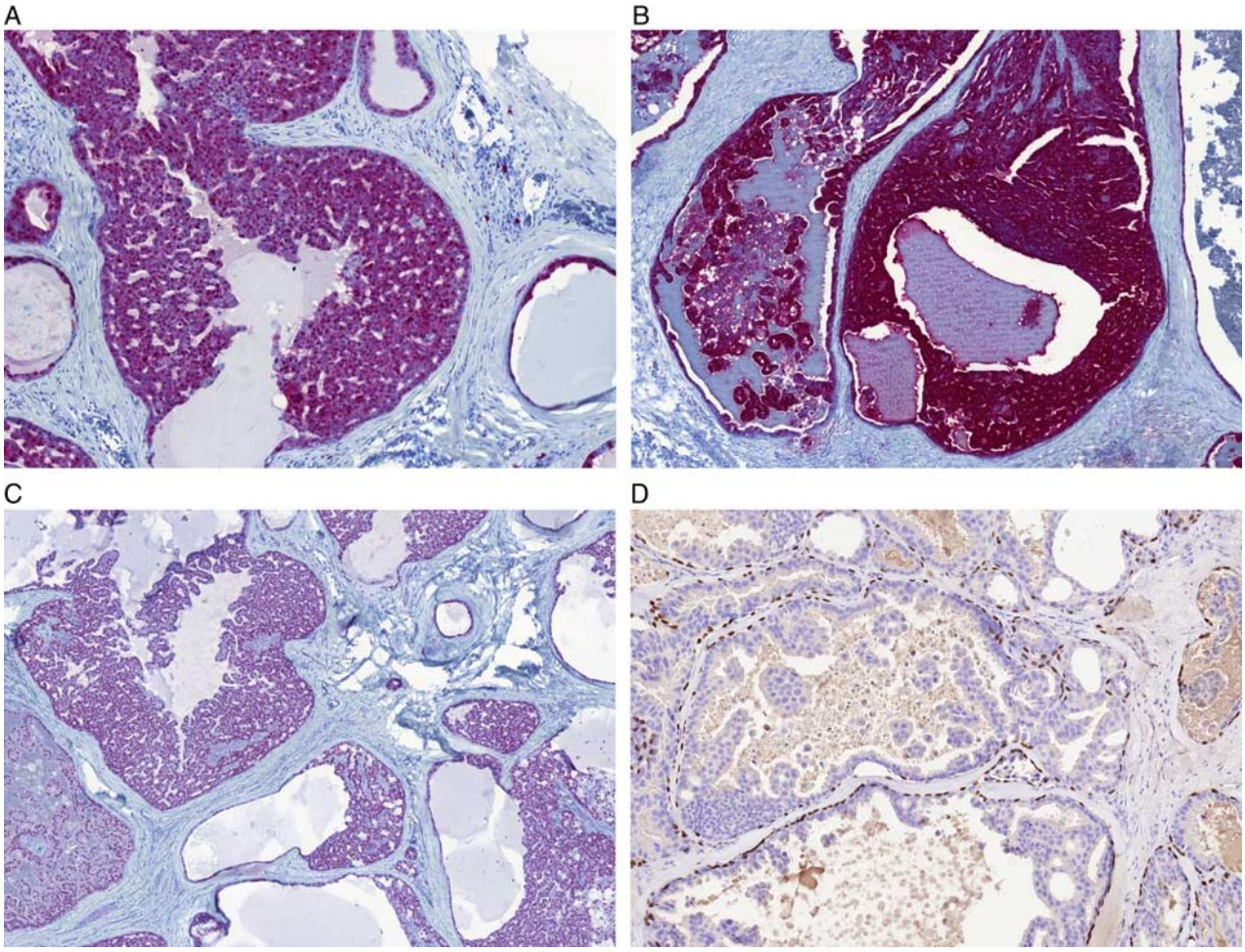


**FIGURE 5.** IC, immunoprofile. IC cases were positive for S100 protein (A), mammaglobin (B), and SOX-10 (C), typically in a strong and diffuse manner. An intact myoepithelial cell layer surrounding tumor islands was evidenced by p63 immunohistochemical expression (which was negative in other tumor cells) (D). Calponin, and CK 14 (D) decorated an intact peripheral myoepithelial cell layer.

In typical cases, IC is noninvasive low-grade carcinoma composed of bland neoplastic cells positive for S100, which is in sharp contrast to SDC. SDC is defined by the recent WHO classification as an aggressive epithelial malignancy resembling high-grade mammary ductal carcinoma; and it is composed of polymorphic cells with S100 negative and AR positive immunoprofile.[20] Therefore these 2 lesions are generally accepted as distinct and separate entities.[19,21,22] Despite this, there are, in the literature, occasional well documented low-grade ICs with subsequent widespread invasion.[10,23] Even more confusing are rare cases of true high-grade SDC reported as purely "in situ lesions."[24]

In recent years, many salivary gland low-grade carcinomas have been found to have pathognomonic translocations and characteristic chromosomal rearrangements. These include *ETV6-NTRK3* and *ETV6-RET* in MASC,[1,8] *MYB-NFIB* and *MYBL1-NFIB* in adenoid cystic carcinoma,[25] *EWSR1-ATF1* in (hyalinizing) clear cell carcinoma,[26] *CRTC1/CRTC3-MAML2* in mucoepidermoid carcinoma,[27] and *PRKD1-3* rearrangements in cribriform adenocarcinoma of tongue and other minor salivary glands.[28] These alterations are tumor-specific and are present in majority of the cases of the given tumor entity. Therefore they may serve as diagnostic markers useful for improvement of salivary gland tumor classification and taxonomy. There have been very few genomic studies to investigate the relationship of carcinomas with prevailing intraductal growth pattern and their morphologies and mimics. In particular, recently Weinreb et al,[10] reported a series of intraductal and invasive carcinomas of intercalated salivary duct origin. They categorized IC into intercalated duct and apocrine phenotype. IC with intercalated duct differentiation harbored a *NCOA4-RET* fusion in one index case and an inversion pattern of *RET* rearrangement by FISH in a subset of cases suggested this may represent a dominant fusion.[10] Only one case in this study showed a classic break-apart pattern with *RET* FISH, suggesting an alternate fusion.[10] In contrast, IC with apocrine phenotype were shown to be negative for *NCOA4-RET*.[10]

In the current study, which is the largest genomic study of IC to date, the *NCOA4-RET* was confirmed to be the dominant fusion in IC, and likely represented all the *RET* positive cases previously reported with an inversion pattern of rearrangement by FISH. A new finding in our study has been a discovery of a subset of IC patients with apocrine variant IC harboring a novel *TRIM27-RET*. The single case with a classic break-apart for *RET* reported by Weinreb et al,[10] was retested in this study and confirmed to harbor *TRIM27-RET*. To our knowledge, *TRIM27--RET* has not been recognized in any other salivary gland tumor so far. A total of 8 of 17 cases (47%) were confirmed to harbor a *RET* fusion. Interestingly, recent studies using RNA sequencing have revealed that SDC may also be added to the growing list of gene fusion-positive salivary carcinomas, with *NCOA4-RET* fusions having been found in 2 SDCs.[29] Both *NCOA4-RET* translocated SDC were positive for AR, and the tumors progressed in spite of undergoing concurrent chemoradiation, combination chemotherapy, and dual androgen deprivation therapy. Both patients with *NCOA4-RET* translocation, however, benefited from *RET*-targeted therapy.[29]

IC has a generally identical immunoprofile with MASC (S100 protein/mammaglobin positive and DOG1/p63 negative in tumor ductal cells with p63 protein immunostaining only in abluminal myoepithelial layer); interestingly MASC (particularly those with *ETV6-RET* gene fusions) seem to closely resemble *NCOA4-RET* translocated ICs by histomorphology as well. Therefore, it is possible that the *NCOA4-RET* gene fusion reported in one case of "MASC" actually represented a case of IC, possibly with invasion concealing its intraductal origin.[11]

In conclusion, NGS analysis of 17 cases of IC detected a *NCOA4-RET* fusion transcript joining exon 7 or 8 of *NCOA4* gene and exon 12 of *RET* gene in 6 cases of intercalated duct type IC; and a novel *TRIM27-RET* fusion transcript between exons 3 and 12 in 2 cases of salivary gland tumors displaying histologic and immunohistochemical features typical of apocrine IC for a total of 47% of IC cases. All analyzed cases were negative for *ETV6-NTRK3* gene fusion by the FusionPlex kit, RT-PCR, and *ETV6* gene was found intact by FISH. A novel finding in our study has been a discovery of a subset of IC patients with apocrine variant IC harboring a novel *TRIM27-RET*. The *RET* negative cases seen in this study and by Weinreb and colleagues, account for half of all ICs. There is likely a non-*RET* fusion or other finding that is not detectable using our current NGS platform and requires further study.

## REFERENCES


1. Skálová A, Vanecek T, Sima R, et al. Mammary analogue secretory carcinoma of salivary glands, containing the *ETV6-NTRK3* fusion gene: a hitherto undescribed salivary gland tumor entity. *Am J Surg Pathol*. 2010;34:599–608.
2. Bishop JA, Yonescu R, Batista D, et al. Most nonparotid "acinic cell carcinomas" represent mammary analog secretory carcinomas. *Am J Surg Pathol*. 2013;37:1053–1057.
3. Chiosea SI, Griffith C, Assaad A, et al. Clinicopathological characterization of mammary analogue secretory carcinoma of salivary glands. *Histopathology*. 2012;61:387–394.
4. Chiosea SI, Griffith C, Assaad A, et al. The profile of acinic cell carcinoma after recognition of mammary analog secretory carcinoma. *Am J Surg Pathol*. 2012;36:343–350.
5. Skalova A, Bell D, Bishop JA, et al. Secretory carcinoma. In: El-Naggar A, Chan JKC, Grandis JR, Takata T, Slootweg PJ, eds. *World Health Organization (WHO) Classification of Head and Neck Tumours*, 4th ed. Lyon, France: IARC Press; 2017:177–178.
6. Ito Y, Ishibashi K, Masaki A, et al. Mammary analogue secretory carcinoma of salivary glands: a clinicopathologic and molecular study including 2 cases harboring *ETV6-X* fusion. *Am J Surg Pathol*. 2015;39:602–610.
7. Skalova A, Vanecek T, Simpson RH, et al. Mammary analogue secretory carcinoma of salivary glands: molecular analysis of 25 *ETV6* gene rearranged tumors with lack of detection of classical *ETV6-NTRK3* fusion transcript by standard RT-PCR: Report of 4 cases harboring *ETV6-X* gene fusion. *Am J Surg Pathol*. 2016;40:3–13.
8. Skálová A, Vanecek T, Martinek P, et al. Molecular profiling of mammary analog secretory carcinoma revealed a subset of tumors harboring a novel *ETV6-RET* translocation: report of 10 cases. *Am J Surg Pathol*. 2018;42:234–246.
9. Loening T, Leivo I, Simpson RHW, et al. Intraductal carcinoma. In: El-Naggar A, Chan JKC, Grandis JR, Takata T, Slootweg PJ, eds. *World Health Organization (WHO) Classification of Head and Neck Tumours*, 4th ed. Lyon, France: IARC Press; 2017:170–171.
10. Weinreb I, Bishop JA, Chiosea SI, et al. Recurrent *RET* gene rearrangements in intraductal carcinomas of salivary gland. *Am J Surg Pathol*. 2018;42:442–452.
11. Dogan S, Benayed R, Chen H, et al. Genomic profiling of the two related "cousins" acinic cell carcinoma and mammary analog secretory carcinoma of salivary glands reveals novel *NCOA4-RET* fusion in mammary analog secretory carcinoma. Abstract USCAP 2017. *Mod Pathol*. 2017;Suppl 30:323A.
12. Bishop JA, Yonescu R, Batista D, et al. Utility of mammaglobin immunohistochemistry as a proxy marker for the *ETV6-NTRK3* translocation in the diagnosis of salivary mammary analogue secretory carcinoma. *Hum Pathol*. 2013;44:1982–1988.
13. Stevens TM, Kovalovsky AO, Velosa C, et al. Mammary analog secretory carcinoma, low grade salivary duct carcinoma, and mimickers: a comparative study. *Mod Pathol*. 2015;28:1084–1100.
14. Shah AA, Wenig BM, LeGallo RD, et al. Morphology in conjunction with immunohistochemistry is sufficient for the diagnosis of mammary analogue secretory carcinoma. *Head and Neck Pathol*. 2015;9:85–95.
15. Chen KT. Intraductal carcinoma of the minor salivary gland. *J Laryngol Otol*. 1983;97:189–191.
16. Delgado R, Klimstra D, Albores-Saavedra J. Low grade salivary duct carcinoma. A distinctive variant with a low grade histology and a predominant intraductal growth pattern. *Cancer*. 1996;78:956–967.
17. Brandwein-Gensler M, Hille J, Wang LJ, et al. Low-grade salivary duct carcinoma: description of 16 cases. *Am J Surg Pathol*. 2004;28:1040–1044.
18. Brandwein-Gensler MS, Gnepp DR. WHO classification of tumours. Low-grade cribriform cystadenocarcinoma. In: Barnes L, Eveson JW, Reichert P, Sidransky D, eds. *Pathology and Genetics of Head and Neck Tumours*. Lyon: IARC Press; 2005:233.
19. Simpson RHW. Salivary duct carcinoma: new developments—morphological variants including pure in situ high grade lesions; proposed molecular classification. *Head Neck Pathol*. 2013;7:S48–S58.
20. Nagao T, Licitra L, Loening T, et al. Salivary duct carcinoma. In: El-Naggar A, Chan JKC, Grandis JR, Takata T, Slootweg PJ, eds. *World Health Organization (WHO) Classification of Head and Neck Tumours*, 4th ed. Lyon, France: IARC Press; 2017:173–174.
21. Cheuk W, Miliauskas JR, Chan JKC. Intraductal carcinoma of the oral cavity. A case report and a reappraisal of the concept of pure ductal carcinoma in situ in salivary gland carcinoma. *Am J Surg Pathol*. 2004;28:266–270.
22. Laco J, Podhola M, Doležalova H. Low-grade cribriform cystadenocarcinoma of the partoid gland: a neoplasm with favourable prognosis, distinct from salivary duct carcinoma. *Int J Surg Pathol*. 2010;18:369–373.
23. Weinreb I, Tabanda-Lichauco R, Van der Kwast T, et al. Low-grade intraductal carcinoma of salivary gland: report of 3 cases

with marked apocrine differentiation. *Am J Surg Pathol*. 2006;30:1014–1021.
24. Simpson RH, Desai S, Di Palma S. Salivary duct carcinoma in situ of the parotid gland. *Histopathology*. 2008;53:416–425.
25. Persson M, Andrén Y, Mark J, et al. Recurrent fusion of MYB and NFIB transcription factor genes in carcinomas of the breast and head and neck. *Proc Natl Acad Sci USA*. 2009;106:18740–18744.
26. Antonescu CR, Katabi N, Zhang L, et al. *EWSR1-ATF1* fusion is a novel and consistent finding in hyalinizing clear-cell carcinoma of salivary gland. *Genes Chromosomes Cancer*. 2011;50:559–570.
27. Tonon G, Modi S, Wu L, et al. t(11;19)(q21;p13) translocation in mucoepidermoid carcinoma creates a novel fusion product that disrupts a Notch signaling pathway. *Nat Genet*. 2003;33:208–213.
28. Weinreb I, Zhang L, Tirunagari LM, et al. Novel *PRKD* gene rearrangements and variant fusions in cribriform adenocarcinoma of salivary gland origin. *Genes Chromosomes Cancer*. 2014;53:845–856.
29. Wang K, Russell JS, McDermott JD, et al. Profiling of 149 salivary duct carcinomas, carcinoma ex pleomorphic adenomas, and adenocarcinomas, not otherwise specified reveals actionable genomic alterations. *Clin Cancer Res*. 2016;22:6061–6068.